Satellite data reveal the 3-D moisture structure of Tropical Intraseasonal Oscillation and its coupling with underlying ocean

Xiouhua Fu, Bin Wang, and Li Tao

International Pacific Research Center (IPRC), School of Ocean and Earth Science and Technology (SOEST), University of Hawai'i at Manoa, Honolulu, Hawaii, USA

Received 3 November 2005; revised 7 December 2005; accepted 21 December 2005; published 3 February 2006.

[1] The water-vapor profiles obtained from the Atmospheric Infrared Sounder (AIRS) on Satellite Aqua are used to document the 3-D moisture structure of the boreal-summer Tropical Intraseasonal Oscillation (TISO) over the Indo-western Pacific region. With the support of several other Satellite data sets, the interactions between the TISO and underlying ocean are also investigated. The AIRS data reveal much larger tropospheric moisture perturbations than those depicted in previous reanalysis and analysis data sets. It also reveals a drying Atmospheric Boundary Layer (ABL) below the TISO convection probably due to the associated downdrafts. Before the occurrence of TISO convection, both positive Sea Surface Temperature (SST) anomaly and ABL moistening are observed. Further analysis suggests that the positive SST anomaly is the major contributor to the ABL moistening through enhancing surface evaporation. Therefore, the intraseasonal SST anomaly could positively feed back to the atmosphere through moistening the boundary layer, destabilizing the troposphere, and contributing to the northeastward propagation of the TISO. **Citation:** Fu, X., B. Wang, and L. Tao (2006), Satellite data reveal the 3-D moisture structure of Tropical Intraseasonal Oscillation and its coupling with underlying ocean, *Geophys. Res. Lett.*, *33*, L03705, doi:10.1029/2005GL025074.

1. Introduction

[2] The Tropical Intraseasonal Oscillation (TISO) is a dominant mode of the Asian-western Pacific summer monsoon. It strongly regulates the monsoon wet and dry spells [*Yasunari*, 1979]. The recurrent nature of the TISO offers an opportunity to predict the envelope of weather beyond the synoptic scale [*Waliser et al.*, 2003a]. State-of-the-art atmospheric general circulation models (GCMs), however, have various problems in realistically representing the TISO, thus hindering the dynamical prediction of intraseasonal variations [*Waliser et al.*, 2003b]. Model problems primarily lie in the inadequate representation of moist convection [*Wang and Schlesinger*, 1999] and probably also in the lack of atmosphere-ocean interactions [*Flatau et al.*, 1997; *Waliser et al.*, 1999; *Fu et al.*, 2003].

[3] *Inness et al.* [2001] suggested that appropriate representation of tropospheric moistening associated with convection plays a critical role in the initiation and maintenance of the TISO. In order to validate the vertical and horizontal structures of moisture in GCMs and further improve the parameterization of moist convection, accurate 3-D observations are needed. Unfortunately, in the active region of the TISO, such as over the tropical Indo-western Pacific Oceans, the available in-situ sounding observations are very limited [*Webster et al.*, 2002].

[4] Satellite remote sensing, on the other hand, offers an excellent alternative to build an observational benchmark of the 3-D water-vapor cycle of the TISO. In this study, we used AIRS data to construct a 3-D moisture cycle associated with the TISO in the Indo-western Pacific region. With the support of several other Satellite data sets, we also explored the mutual interactions between the TISO and underlying sea surface, particularly focusing on the physical processes through which intraseasonal SST anomalies could feed back to the TISO.

2. Data Sets

[5] Satellite Aqua, the second Earth Observing System polar orbiting platform, was launched with the AIRS in late 2002. The AIRS, with wide spectral coverage in four diverse bands, has the ability to observe 3-D weather from the surface through clouds to the top of the atmosphere. AIRS data provide unprecedented global 3-D distributions of moisture and temperature with very high spatial-temporal resolutions (more description of AIRS instrument, products, and validation is given by B. Tian et al. (Vertical moist thermodynamic structure and spatial-temporal evolution of the Madden-Julian Oscillation based on the atmospheric infrared sounder data, submitted to *Journal of Atmospheric Science*, 2005)). In this study, we used data from two recent years (2003 and 2004).

[6] To further explore the possible feedback of intraseasonal SST anomalies onto the TISO, several other Satellite data sets were also used. They include the SST from Aqua/AMSR_E, rainfall from GPCP, and surface wind from QuikSCAT. Original AIRS data have twice-daily observations (ascending and descending path). They were averaged into 5-day (i.e. pentad) mean data. All other data sets were also averaged from daily into pentad-mean data. In the following analyses, all data sets were filtered to retain only the intraseasonal variability with periods of 20–70 days.

3. Results

[7] This study focuses on the TISO during boreal summer (May–Oct) in the Indo-western Pacific sector. The filtered rainfall time series averaged in the Eastern Indian Ocean (EIO, 5°S–5°N, 80°E–100°E) were used to select the TISO events because this region is identified as an amplification and initiation region for the TISO [*Wang and*

0094-8276/06/2005GL025074$05.00

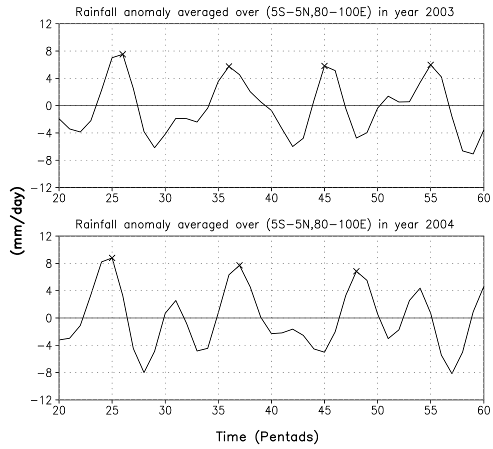

Figure 1. Intraseasonal (20–70-day) rainfall anomalies (mm day^{-1}) averaged over the central-eastern Indian Ocean (5°S–5°N, 80°E –100°E) in summers of (a) 2003 and (b) 2004. Seven intraseasonal events (with their peaks highlighted) have been selected to construct a composite TISO cycle.

Rui, 1990; *Fu and Wang*, 2004]. In total, 7 TISO events were selected from two recent years (Figure 1). In the following study, composite results of all 7 TISO events are presented.

3.1. The TISO-SST Interaction

[8] The composite TISO cycle in Figure 2 reveals coherent space-time evolutions of intraseasonal rainfall, SST and surface wind anomalies in the Indo-western Pacific region. Four pentads before the rainfall peaks in the EIO, the central-eastern Indian Ocean and Maritime Continent are dominated by the suppressed phase (Figure 2a). The dry spell produces positive SST anomalies in the equatorial Indian Ocean through increasing downward solar radiation and decreasing latent heat flux [*Sengupta and Ravichandran*, 2001]. At the same time, positive rainfall anomalies are observed in the western North Pacific (WNP), Bay of Bengal, eastern Arabian Sea and western equatorial Indian Ocean (WIO). As suggested by *Wang et al.* [2005], the positive rainfall in the WIO is likely initiated by the suppressed phase through warming up the sea surface and generating surface convergence with the associated equatorial easterly (Figure 2a).

[9] In the following two phases (Figures 2b–2c), the dry zone in the EIO gradually moves northeastward with negative SST anomalies at its leading edge. The convection initiated in the WIO moves eastward and reaches maximum in the EIO, leaving a negative SST anomaly patch behind. When the positive rainfall anomaly reaches the Maritime Continent, it bifurcates and moves off equatorial region with positive SST anomalies at the leading edges in both the North and South Hemispheres (Figure 2d). The SST anomalies in the NH are much larger than their counterparts in the SH. This may partly account for the quick decay of the southward branch of the positive rainfall anomalies (Figure 2e).

[10] The observed coherent evolutions of the TISO-related rainfall, surface wind and SST anomalies suggest that the TISO and SST feedback to each other positively. It is commonly accepted that the observed intraseasonal SST anomalies are primarily forced by the surface heat-flux changes associated with the TISO [*Wang and Xie*, 1998; *Sengupta and Ravichandran*, 2001]. On the other hand, whether and how the intraseasonal SST anomalies feed back to the TISO is somewhat controversial [*Hendon*, 2000] although many modeling studies have suggested that including TISO-related SST fluctuations in an atmospheric model improves the simulations of the TISO [e.g., *Flatau et al.*, 1997; *Waliser et al.*, 1999; *Fu et al.*, 2003]. Because of the large-scale nature of the intraseasonal variations and the extremely sparse in-situ observations available in the Indo-western Pacific Oceans, it is very difficult to unravel the feedback processes of intraseasonal SST anomalies with the in-situ observations [*Webster et al.*, 2002].

[11] Using the Satellite retrieved atmospheric boundary-layer (ABL) humidity and SST, the possible atmospheric responses to intraseasonal SST anomaly are revealed in this section. Some previous studies [e.g., *Lau and Sui*, 1997] have suggested that the intraseasonal SST anomaly could feed back to the atmospheric convection through modifying the atmospheric convective instability. If this is the case, we should be able to detect the impact of SST anomaly on the ABL moisture with the Satellite observations. To examine this hypothesis, the composite space-time evolutions of

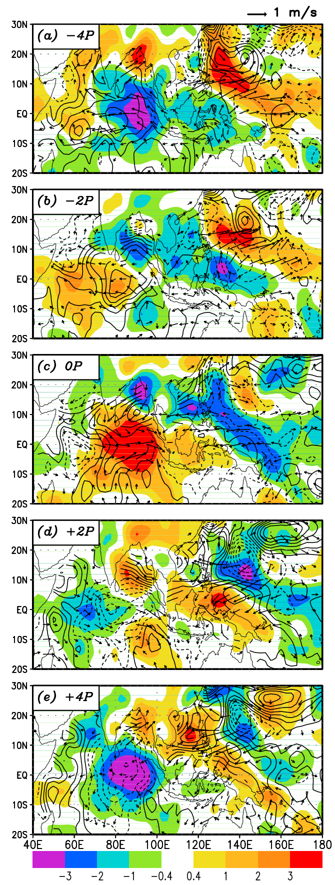

Figure 2. Composite space-time evolutions of rainfall (color shaded, mm day^{-1}), SST (contour interval: 0.1°C), and surface wind (m s^{-1}) anomalies of seven intraseasonal events at (a) −4 pentads, (b) −2 pentads, (c) 0 pentad, (d) +2 pentads, and (e) +4 pentads. The rainfall is from GPCP data set; SST from Aqua/AMSR_E; and surface wind from QuikSCAT.

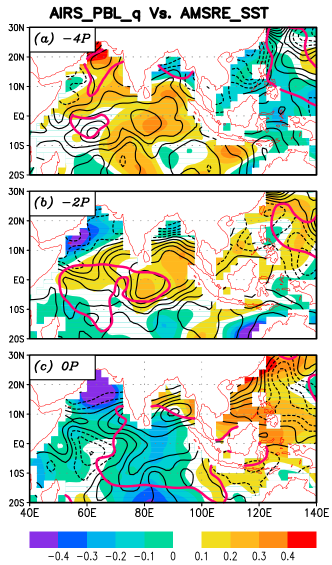

Figure 3. Composite space-time evolutions of atmospheric boundary-layer specific humidity (shaded, g kg^{-1}), SST (contours, CI: 0.1°C), and rainfall (thick red contours with the value of 1 mm day^{-1}) anomalies at (a) −4 pentads, (b) −2 pentads, and (c) 0 pentad. The specific humidity is from AIRS data set.

SST, ABL specific humidity and rainfall anomalies associated with the onset and development of the TISO convection are examined. Figures 3a–3c shows that the positive SST anomaly forms in the WIO and extends eastward, so does the positive ABL moisture anomaly. In this period, positive ABL moisture anomaly almost collocates with positive SST anomaly in the leading edge of the TISO convection. On the other hand, negative ABL moisture anomaly is observed underneath and behind of the convection. This result suggests that the positive SST anomaly moistens the ABL and the convection acts to dry the ABL, particularly over the Indian Ocean. Because the ABL is usually a well-mixed layer, its moistening could be attributed to two factors: surface convergence and evaporation. In the next section, we will see that surface convergence is not a major factor for the observed ABL moistening during this period. Therefore, the enhanced evaporation by the positive SST anomaly might be the dominant contributor.

3.2. Vertical Structure

[12] Figure 4 shows the composite height-latitude moisture perturbations along with the rainfall, surface convergence and SST anomalies during the onset and development of the TISO convection averaged between 85°E and 95°E. This period also features the transition from eastward to northward propagation of the TISO within this longitudinal band. At −2 pentads (Figure 4a), the TISO convection does not reach this band yet but surface convergence obviously exists between 5°S and 7°N, indicating that the surface convergence leads the eastward-propagating TISO as found before [*Wang and Li*, 1994]. Positive ABL moisture perturbations are observed between 10°S and 15°N with the maximum shifting to the NH. Apparently, surface moisture convergence can't explain all the observed ABL moistening particularly north of 7°N. The positive SST anomaly, however, appears from 10°S to about 15°N and could account for the positive ABL moisture perturbation north of 7°N through enhancing surface evaporation [*Shinoda et al.*, 1998].

[13] At next two pentads (Figure 4b–4c), the deep convection reaches this longitudinal band with maximum rainfall near the equator. The entire troposphere has been

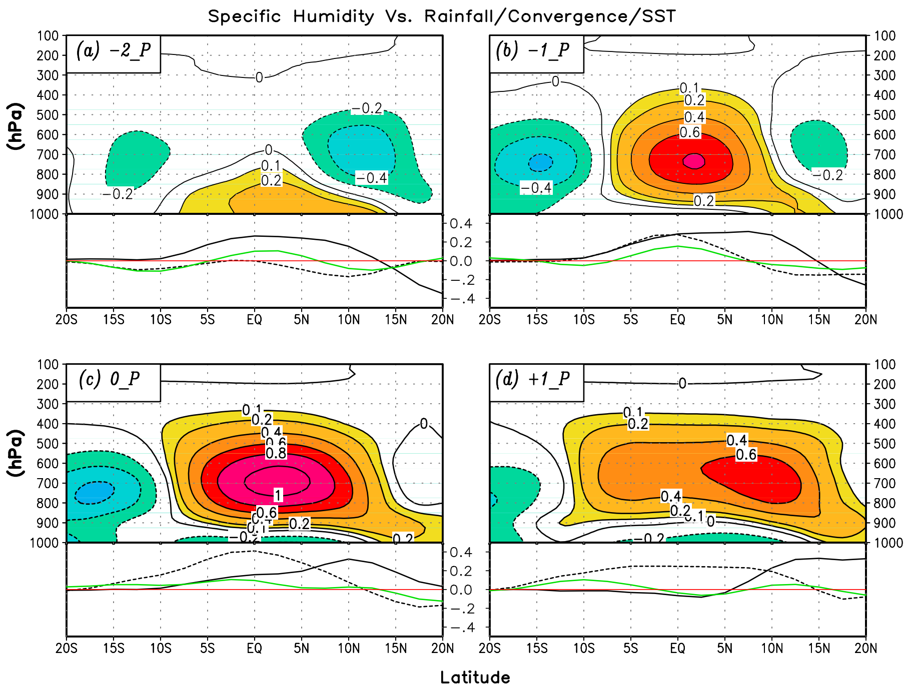

Figure 4. Composite height-latitude plots of specific humidity (g kg^{-1}) anomalies averaged over 85°E–95°E along with composite rainfall (black-dashed line, unit: 20 mm day^{-1}), SST (black-solid line, unit: °C) and surface convergence (green-solid line, unit: 5×10^{-6} s^{-1}) anomalies at (a) −2 pentads, (b) −1 pentad, (c) 0 pentad and (d) +1 pentad.

moistened with a maximum near 700-hPa. Convection tends to dry the ABL probably through the associated downdrafts. The ABL moistens up in the north of the convection. Similar as before, this ABL moistening can't be explained by surface convergence, which is almost collocated with the convection. On the other hand, the ABL moistening is always associated with positive SST anomalies. At 0 pentad (Figure 4c), the maximum tropospheric moisture perturbation reaches 1 g kg^{-1} near 700-hPa. This value is much larger than those revealed by the ECMWF analysis ($\sim$0.2 g kg^{-1}) [*Fu and Wang*, 2004, Figure 12] and by NCAR/NCEP reanalysis ($\sim$0.6 g kg^{-1} in the ABL) [*Jiang et al.*, 2004, Figure 8]. None of the ECMWF analysis and NCEP reanalysis has shown any negative ABL moisture anomalies underneath the deep convection. At +1 pentad (Figure 4d), both the maximum positive rainfall and tropospheric moisture anomalies have shifted to the NH. The positive SST anomaly and the accompanying ABL moistening are still ahead of the TISO-related deep convection in between 15°N and 20°N.

4. Summary and Discussion

[14] Our analysis indicates that the TISO-related tropospheric moisture perturbations in the AIRS data set are much larger than those depicted with previous ECMWF analysis and NCAR/NCEP reanalysis. Both of them have been widely used as observations to validate models. If the AIRS data are closer to the ground truth, many state-of-the-art GCMs may considerably underestimate the tropospheric moisture perturbations associated with the TISO convection. The AIRS data also reveal a drying atmospheric boundary layer associated with the convection. This feature doesn't exist in the previous analysis and reanalysis data sets, but appears in some sounding observations [e.g., *McBride and Frank*, 1999, Figure 4]. This may suggest that the impact of convection-induced downdrafts on the ABL is significantly underestimated in both ECMWF and NCEP reanalysis data sets.

[15] The coherent evolutions of the TISO-related rainfall, surface wind and SST anomalies suggest that the TISO and SST positively feed back to each other. This study provided a piece of observational evidence to support that the intraseasonal SST anomalies feed back to the TISO positively. The suppressed phase of the TISO generates positive SST anomalies in the equatorial and northern Indian Ocean (Figure 3). These SST anomalies moisten the atmospheric boundary layer most likely by enhancing surface evaporation (Figure 4). The moistened ABL ahead of the convection will destabilize the atmosphere and help the TISO-related convection propagate northeastward. Given that only 7 TISO events over 2 summers were used to construct the composite TISO cycle in this study, apparently, further studies as new data become available are warranted.

[16] In order to quantify the contribution of intraseasonal SST anomalies on the ABL moistening and its feedback to the TISO, future researches are needed to obtain the high-frequency surface evaporation associated with intraseasonal SST anomalies; and to estimate the relative contributions of surface convergence and evaporation on ABL moistening through moisture budget analysis. Evidently, more coordinated surface and boundary-layer observations in the Indo-western Pacific Oceans are needed to conduct the proposed studies.

[17] **Acknowledgments.** This work was supported by NASA Earth Science Program and NSF Climate Dynamics Program and by the Japan Agency for Marine-Earth Science and Technology (JAMSTEC) through its sponsorship of the IPRC. The AIRS data set was kindly provided by the AIRS Science Team at NASA JPL. This paper is SOEST contribution number 6705 and IPRC contribution number 366.

References

Flatau, M., P. Flatau, P. Phoebus, and P. Niller (1997), The feedback between equatorial convection and local radiative and evaporative processes: The implications for intraseasonal oscillations, *J. Atmos. Sci.*, *54*, 2373–2386.

Fu, X., and B. Wang (2004), The Boreal-Summer Intraseasonal Oscillations simulated in a hybrid coupled atmosphere-ocean model, *Mon. Weather Rev.*, *132*, 2628–2649.

Fu, X., B. Wang, T. Li, and J. P. McCreary (2003), Coupling between northward-propagating, intraseasonal oscillations and sea surface temperature in the Indian Ocean, *J. Atmos. Sci.*, *60*, 1733–1753.

Hendon, H. H. (2000), Impact of air-sea coupling on the Madden-Julian Oscillation in a general circulation model, *J. Atmos. Sci.*, *57*, 3939–3952.

Inness, P. M., J. M. Slingo, S. J. Woolnough, R. B. Neale, and V. D. Pope (2001), Organization of tropical convection in a GCM with varying vertical resolution; Implications for the simulation of the Madden-Julian Oscillation, *Clim. Dyn.*, *17*, 777–793.

Jiang, X., T. Li, and B. Wang (2004), Structures and mechanisms of the northward propagating boreal summer intraseasonal oscillations, *J. Clim.*, *17*, 1022–1039.

Lau, K. M., and C.-H. Sui (1997), Mechanisms of short-term sea surface temperature regulation: Observations during TOGA COARE, *J. Clim.*, *10*, 465–472.

McBride, J. L., and W. M. Frank (1999), Relationships between stability and monsoon convection, *J. Atmos. Sci.*, *56*, 24–36.

Sengupta, D., and M. Ravichandran (2001), Oscillations of Bay of Bengal sea surface temperature during the 1998 summer monsoon, *Geophys. Res. Lett.*, *28*, 2033–2036.

Shinoda, T., H. H. Hendon, and J. Glick (1998), Intraseasonal variability of surface fluxes and sea surface temperature in the tropical western Pacific and Indian oceans, *J. Clim.*, *11*, 1685–1702.

Waliser, D. E., K. M. Lau, and J. H. Kim (1999), The influence of coupled sea surface temperatures on the Madden-Julian Oscillation: A model perturbation experiment, *J. Atmos. Sci.*, *56*, 333–358.

Waliser, D. E., W. Stern, S. Schubert, and K. M. Lau (2003a), Dynamic predictability of intraseasonal variability associated with the Asian summer monsoon, *Q. J. R. Meteorol. Soc.*, *129*, 2897–2925.

Waliser, D. E., et al. (2003b), AGCM simulations of intraseasonal variability associated with the Asian simmer monsoon, *Clim. Dyn.*, *21*, 423–446.

Wang, B., and T. Li (1994), Convective interaction with boundary-layer dynamics in the development of a tropical intrasaesonal system, *J. Atmos. Sci.*, *51*, 1386–1400.

Wang, B., and H. Rui (1990), Synoptic climatology of transient tropical intraseasonal convection anomalies: 1975–1985, *Meteorol. Atmos. Phys.*, *44*, 43–61.

Wang, B., and X. Xie (1998), Coupled modes of the warm pool climate system. part I: The role of air-sea interaction in maintaining Madden-Julian Oscillation, *J. Clim.*, *11*, 2116–2135.

Wang, B., P. J. Webster, and H. Teng (2005), Antecedents and self-induction of active-break south Asian monsoon unraveled by satellites, *Geophys. Res. Lett.*, *32*, L04704, doi:10.1029/2004GL020996.

Wang, W., and M. E. Schlesinger (1999), The dependence on convection parameterization of the Tropical Intraseasonal Oscillation simulated by the UIUC 11-layer atmospheric GCM, *J. Clim.*, *12*, 1423–1457.

Webster, P. J., et al. (2002), The JASMINE Pilot Study, *Bull. Am. Meteorol. Soc.*, *83*, 1603–1629.

Yasunari, T. (1979), Cloudiness fluctuations associated with the Northern Hemisphere summer monsoon, *J. Meteorol. Soc. Jpn.*, *57*, 227–242.

X. Fu, L. Tao, and B. Wang, IPRC, SOEST, University of Hawai'i at Manoa, 1680 East West Road, 401 POST Bldg., Honolulu, HI 96822, USA. (xfu@hawaii.edu)